Accurate Body Temperature Measurement of a Neonate Using Thermography Technology

Rassels, Kianoush; French, Paddy

DOI
10.1109/SSI52265.2021.9467024

Publication date
2021

Document Version
Accepted author manuscript

Published in
Proceedings of the Smart Systems Integration, SSI 2021

Accurate Body Temperature Measurement of a Neonate Using Thermography Technology

Kianoush Rassels
BioMechanical Engineering
TU-Delft
Delft, The Netherlands
K.Rassels@tudelft.nl

Paddy French
Bioelectronics Research Group
TU-Delft
Delft, The Netherlands
P.J.French@tudelft.nl

***Abstract*—One of the important measured vital signs in neonates is the body temperature. The traditional measurement uses adhesive pads, but medical staff are hindered by connectors attached to the infant. Remote infrared thermal imaging techniques provide a non-intrusive and safe method to measure body temperature. By means of the thermography technology, it is possible to monitor the variations and trends in the body temperature, which is more reliable, faster, less stressful than traditional methods. Measuring body temperature of a moving neonate remains a challenge. Moreover, factors like humidity, thermal lens forming through the incubator portholes, thermal noise from inside and outside the incubator, camera position and limited Field of View through the incubator portholes, etc. could disrupt a reliable measurement. This study will focus on developing a technique that measures neonates' body temperature accurately in an incubator. By eliminating unwanted external factors, continual measurement of a Region of Interest (ROI) become more feasible from which trends become available for the techniques like Artificial Intelligence, Machine Learning or Deep Learning. Moreover, this method reduces stress and discomfort for the infant. The outcome of this study is more accurate and the temperature profile of a geometric shapes or ROI over time provides a valuable input to the physicians or nurses to provide higher quality care.**

Keywords—Thermography technology, neonates, body temperature, infrared thermal imaging, incubator, temperature measurement.

I. Introduction

Preterm or neonate is a baby born at fewer than 37 weeks About 15 million of the neonates (5%~18%) across 184 countries born in premature condition [2]. These preterm babies can be divided into more sub-categories: moderately to late preterm (32-37 weeks), very preterm (28-32 weeks), and extremely preterm (<28 weeks). Preterm babies are more susceptible to diseases because their organs and immune system are not fully developed. Therefore, they are usually kept in an incubator. The skin regulates body temperature and has sensory preceptor and protects the body against UV radiation and pathogens. However, these functions are not fully developed for neonates. After birth and during the first year, the skin is very fragile and needs to develop these functions till it reaches maturity. For premature babies, this development starts from the 2nd or 3rd week after birth [3]. In most hospitals, skin sensors are used, but these may damage the fragile and sensitive skin of preterm neonates and increase the risk of infection [4, 5]. The removal of skin sensor also increases transepidermal water loss (TEWL) at the sensor location, which is correlated with damaged skin barrier function [6]. Another concern due to the thin corneum stratum is that the skin is highly permeable to topically applied agents, which if absorbed, can cause toxic systemic effects and lead to illness or even death [7]. Similarly, repeatedly applying disinfectant such as isopropyl alcohol to neonate skin can induce systemic intoxication and can cause severe haemorrhagic skin necrosis [8].

Body temperature of a neonate provides a much information on health of the baby (e.g. adverse condition) [9-11], hence an accurate thermal measurement would really benefit the baby. Current temperature measurements for the neonate are in rectum, axilla, ear, and forehead, with rectal and axillary thermal measurement frequently regarded as the golden standard [12–14]. However, these measurements are not ideal for the baby and could cause distress. Other disadvantages such as perforation of the rectum, infection/hygienic concern, and irritation also cause some concerns for rectal thermometer [15, 16]. For axillary thermometer, babies have to be in a certain position or handled in such a way in order to get accurate measurement. These measurements are not continuous. For continuous temperature measurement, a skin temperature a sensor is used, but these have the downside of skin damage and increasing infection risk. Our focus in this paper is to measure neonate's body temperature by means of an infrared thermal imaging that are kept in an incubator.

II. Incubator Environment

A. Incubator Environment

Neonates mostly are kept in incubators, since their internal body temperature mechanisms are underdeveloped. It is crucial that neonates do not lose excessive heat or get too warm. In order to guard them against hypothermia or hyperthermia, they are often placed in an incubator. Different incubators like Giraffe Incubator Carestation, have features like air control mode, baby temperature control mode as main features, and humidity control, and oxygen level control as optional features to create an optimal. The environment is generally controlled by fan to circulate the air inside the incubator, servocontrol to control the heater, water dispenser for humidifying the incubator, and oxygen valve. Heat exchange between the environment and the neonate happens by convection of the air to the skin of the baby. Air temperature colder than the skin of the neonate would result in convective heat loss due to the velocity of the air flow. Higher velocity would mean higher heat transfer from the skin to the environment. However, this low air flow also does reduce the ability to warm hypothermic neonates as quickly as possible [17].

Smart Systems Integration Conference SSI2021
April 27th -29th, 2021, Grenoble/ France
XXX-X-XXXX-XXXX-X/XX/$XX.00 ©20XX IEEE

III. Thermal Imaging

A thermal camera can register the spatial and temporal variations in temperature receiving from an object and provide thermal information. The infrared spectrum is shown in Fig. 1. However, thermal imaging technique usually detects long-infrared radiation with a wavelength range from 9 to 14 µm to create radiation images.

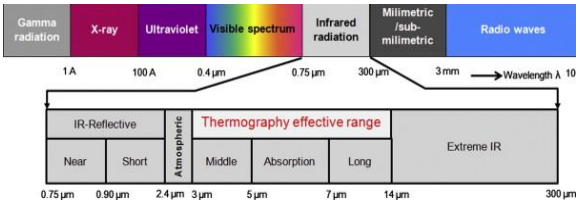

Fig. 1. Infrared region within electromagnetic spectrum [19].

Human body emits significant radiations of wavelength in range 4 to 30 µm, with peak at 9 µm [18], which is suitable for the thermal imaging. Depending on the clinical questions a thermal camera can be used to measure temperature variations or differences for diagnostics purposes. An incubator is a controlled environment, and the thermal images of preterm infants are being affected by the incubator environment [1]. The hood of the incubator is generally made out of polymethyl methacrylate (PMMA) (also known as acrylic or plexiglass) or polycarbonate. Unfortunately, these materials are very poor for infrared wave transmission, so thermal radiation range cannot look through these materials [20].

IV. Experimental Setup

A. Hardware and Software

In this research, a FLIR SC305 infrared camera connected to a Pine RockPro64 Single Board Computer (SBC) have been used, see Fig. 2.

The SBC specs are: a Rockchip RK3399 hexa-core System on Chip (SOC) as well as a quad-core Mali-T860MP4 with 4GB of dual-channel LPDDR4 system memory. The measurements are done with 9 Hz frame rate and a resolution of 320x240 pixels.

The infrared camera is linked with a dedicated software to capture thermal images. Through the software, live stream of the camera can be seen and analysed in real-time. Temperature of each pixel or region can be displayed and object parameter settings such as emissivity, distance, and more can be modified. Filters can also be applied to the image or video through this software

The radiant energy emitted from object in the form of infrared wave is captured and measured by this infrared camera. Thereafter, by means of a certain formula(s) defined by the manufacturer the temperature of the object is being calculated after compensation of environment variables, such as atmospheric temperature, distance, humidity, etc. affecting the object radiance.

Fig. 2. FLIR SC305 infrared camera & Pine RockPro 64 (SBC).

B. Temperature Measurements Setup

Different temperature measurement setup can be considered; 1- Placing the camera lens inside a tightly fitting gap through one of the port holes of the incubator, 2- Placing the camera above the hood at 90˚ angel, 3- Placing the camera in front of opening (port hole) of the incubator, 4- Placing the camera in the incubator. Each measurement setup has its own (dis-)advantages and it is able to avoid, or deal with radiation or thermal noise sources. In all possible setup scenario's, the field of view of the infrared camera has to be clear as incubator's Plexiglas hood is completely opaque to IR. In this study, measurement setup (3) has been chosen from the practical point of view and in consultation of the physicians and nurses who provide care to the neonates. Placing the Infrared camera in front of opening (port hole) and in some distance from of the incubator does not interfere with care providers' daily work, which is of importance in life threatening situations.

Using measurement setup (3); a generalized model of thermal measurement of neonate inside an incubator is shown in the Fig. 3, ref. [1].

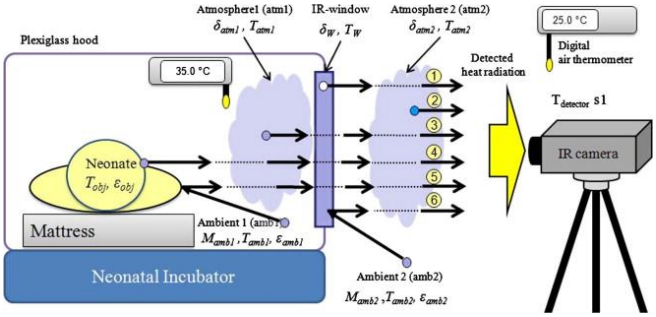

Fig.3. Thermal measurement of neonate inside incubator with an infrared camera [1].

The temperature measured by the camera is being influenced by 6 sources of radiation, namely: 1- Atmosphere temperature outside the incubator, 2- Atmosphere temperature inside the incubator, 3- Neonate's actual body temperature, 4- Infrared window (An open port hole), 5- Reflections from ambient objects inside the incubator, and 6- Reflections of ambient objects outside the incubator.

In case, the port hole of the incubator is being covered by an infrared transparent foil like polyehtylene (PE), the radiation sources 4 and 6 can be discarded.

From the model shown in the Fig. 3Fig., following equation can be written [1]:

$$T_{detector} = \frac{T_{obj}}{\varepsilon_{obj}\cdot\delta_{atm1}\cdot\delta_{\omega}\cdot\delta_{atm2}} + \frac{(1-\varepsilon_{obj})\cdot T_{amb1}}{\varepsilon_{obj}} + \frac{(1-\delta_{atm1})\cdot T_{atm1}}{\varepsilon_{obj}\cdot\delta_{atm1}} + \frac{\varepsilon_{\omega}\cdot T_{\omega}}{\varepsilon_{obj}\cdot\delta_{atm1}\cdot\delta_{\omega}} + \frac{R_w\cdot T_{amb2}}{\varepsilon_{obj}\cdot\delta_{atm2}\cdot\delta_{\omega}} + \frac{(1-\delta_{atm1})\cdot T_{atm2}}{\varepsilon_{obj}\cdot\delta_{atm1}\cdot\delta_{\omega}\cdot\delta_{atm2}} \quad (1)$$

where variables T, ε, δ and R are temperature, emissivity, transmittance, and reflectance respectively and subscripts as: *obj* = object measured, *amb1* and *amb2* as ambient object

inside and outside the incubator, *atm1* and *atm2* as atmosphere inside and outside incubator, and *w* as infrared window.

C. Measurement Error

Different sources of measurement errors can contribute and distort the actual neonate's body temperature measured by the infrared camera. These errors could be caused by measurement setup, calibration error, and electronic path error of the device and detector noise of the IR camera. The errors from the measurement setup are coming from incorrect evaluation of object emissivity, ambient temperature, atmospheric temperature, relative atmospheric humidity, distance from camera to object, and atmospheric transmission and radiance [19].

Based on the general model from Fig. 3 and experiments the total error budget for a thermal imaging measurement on neonates inside an incubator is modelled in (2):

$$T_{error} = \frac{\Delta\varepsilon}{0.245}\times 0.01T_{obj} + \frac{\Delta T_{ambient}}{8.8K}\times 2.2\times 10^{-3}T_{obj} + \frac{\Delta T_{atmosphere}}{8.8K}\times 5\times 10^{-4}T_{obj} + \frac{\Delta d}{30m}\times 3\times 10^{-4}T_{obj} + \frac{\Delta\omega}{15\%}\times 3\times 10^{-4}T_{obj} + T_n + T_l + T_c \quad (2)$$

where T_{error} is the total temperature error of the measurement, T_{obj} is the actual temperature of the object, ε is emissivity of the object, $T_{ambient}$ is the temperature of objects around the measured object, $T_{atmosphere}$ is the atmospheric temperature, d is distance of object from camera, ω is relative humidity of the environment, T_n is thermal noise from the camera, T_l is thermal lens forming error at the port holes of the incubator, and T_c is the calibration and electronic path error with the constants derived from error simulation in Infrared Thermography: Errors and Uncertainties [19].

D. Contribution of Thermal Lens at the port holes

Due to experimental setup described in Fig.3, the port hole of the incubator is open and there is an exchange of hot air to cold air from inside of the incubator to the room. This flow or turbulence of hot and cold air with difference in refractive index did not form an invisible thermal convex of concave lens, mirage, or distorted temperature along the path of sight at the port hole as such affecting the temperature measurement by the infrared camera. This was investigated using Pyramidal implementation of the Lucas Kanade feature tracker scaling and Gunnar Farneback Optical Flow algorithms, [21] and [22], respectively with the following parameters; image scale=0.5, number of pyramid layers=10, averaging windows size=20, number of iterations for each pyramid level=10, size of the pixel neighbourhood used to find the polynomial expansion=10, standard deviation=5.0. To investigate the existence of the thermal lens forming at the port holes, the linear dependency of the angle and direction of the optical flow pixels are calculated by Pearson correlation coefficient (3).

$$\rho(A,B) = \frac{1}{N-1}\sum_{i=1}^{N}\left(\frac{A_i-\mu_A}{\sigma_A}\right)\left(\frac{B_i-\mu_B}{\sigma_B}\right) \quad (3)$$

where μA and σA are the mean and standard deviation of direction pixel matrix A, respectively, and μB and σB are the mean and standard deviation of direction pixel matrix B. The result of the function is a correlation coefficient matrix for each pairwise combination.

$$R = \begin{pmatrix} \rho(A,A) & \rho(A,B) \\ \rho(B,A) & \rho(B,B) \end{pmatrix} \quad (4)$$

Since a variable is always correlated to itself, the diagonal entry of the matrix will always be 1.

$$R = \begin{pmatrix} 1 & \rho(A,B) \\ \rho(B,A) & 1 \end{pmatrix} \quad (5)$$

Moreover, the movement of each pixel is shown in an angle grouped histogram to show which direction the pixels dominantly moving to investigate thermal lens forming, Fig. 4.

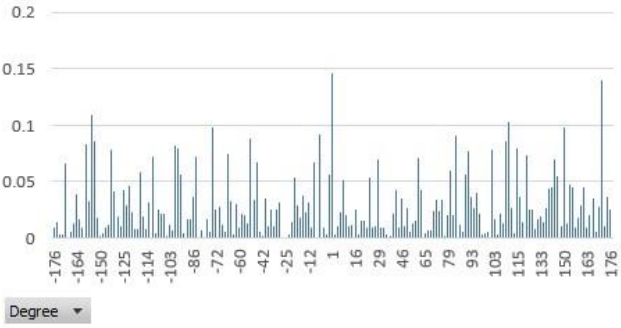

Fig. 4. Histogram of optical flow pixel movement grouped by angle.

The experiments on all port holes resulted in correlation coefficient well below 0.2, indicating that there is random or little pattern in the pixel movement on the video. The movement of the pixels are mostly caused by noise in the measurement. Based on the results, it is concluded that there is no evidence of air flow or turbulence in the porthole affecting the measurement of the infrared camera. The snapshot of processed video output in Fig. 5; right, shows visualized optical flow containing sequential angle.

In other words, the angle and the magnitude of the optical flow pixels do not show linear dependency as such that thermal lens forming can be justified by the exchange of the hot air inside the incubator and the cold air from the room.

From the error budget (2), most contribution of the 5 environmental variables (e.g., emissivity, ambient, atmosphere temperature, distance, and humidity), is coming from the emissivity and ambient temperature. However, as the emissivity of human body is known, thus emissivity setting error is negligible, leaving ambient temperature as the major error contributor in (2).

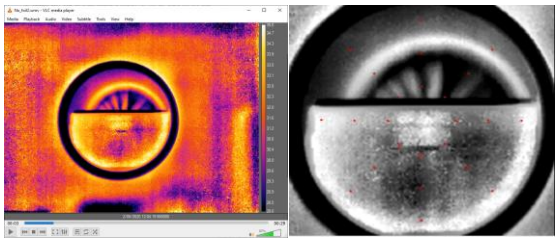

Fig. 5. Left: A snapshot of the incubator port hole, right: random behavior of the dense optical flow (with different magnitudes and directions) showing no thermal lens forming at the port holes of the incubator.

E. Thermal Noise Compensation

In (2), the combination of errors contributing to the total error budget is discussed; 1- Emissivity error, 2- ambient temperature error, 3- atmospheric temperature error, 4- distance error, 5- relative humidity error, 6- camera thermal noise; e.g. angle error, thermal lens forming error, and calibration and electronic path error). As discussed, contribution of some errors is much smaller compared to other errors, hence they could be neglected. The emissivity error has most contribution in total error budget. However, its contribution is constant up to 45° from the surface normal angle of observed object and it will increase in value when the angle is increased [23, 24]. As the diameter of incubator portholes varies from 15cm to 20cm, with the infrared camera 1m to 2m away from the porthole, the viewing angle of the camera is below 45°, hence the emissivity setting can be set to 0.97-0.98 and the error can be neglected.

Ambient temperature setting error has the second highest contribution in (2). Ambient temperature is used to compensate reflections coming from other objects around the measured object. In the practice, the reflection may come from the incubator walls, or walls and objects outside the incubator if the incubator cover is removed. The variability of the reflected object temperature is contributing the most to the temperature error. The experiments show that the difference between incubator wall temperature and room temperature may be as high as 10 °C. This amount of deviation in the setting will result in temperature error of around 0.7 °C.

Atmospheric temperature error has a small contribution error in (2). In the practice, the room temperature where the baby and incubator are located, is relatively stable, which results in that the incubator air temperature will also be relatively stable. A change in the atmosphere temperature of 4 °C would only yield temperature error under 0.1 °C. So, the atmospheric temperature can be set to room temperature and the error can be neglected in the practice.

The distance between the camera and baby is relatively the same (e.g. around 1 metre) for every measurement. The distance variation between 1m to 2 meters would yield an error below 0.01 °C. Hence, distance error is also considered negligible.

For the relative humidity, nurse and doctors almost never use humidifier of the incubator, so the humidity inside the incubator will not change as such. This research was limited for the humidity up to 80%.

The experiments showed, camera's thermal noise causes fluctuation in the reading of the temperature along with humidity of environment. The total value is measured around ±0.15 °C for our FLIR camera, which is random in nature. Since calibration error and electronic path error of the camera are part the hardware, this total error needs to be compensated as offset error compensation. This offset value can be determined using a Wahl ambient temperature blackbody and a pre-calibrated PT100 temperature sensor used inside an aluminium block to avoid temperature variations during different experiments.

After elimination of error sources which do not have significant contribution in the total to be calculated temperature error, (2) can be simplified to (6):

$$T_{error} = \frac{\Delta T_{ambient}}{8.8K} \times 2.2 \times 10^{-3} T_{obj} + T_{Thermal\,noise} + T_{offset} \quad (6)$$

Ambient temperature error will be compensated with the formula shown. The ambient temperature can be obtained by having a temperature sensor placed on the wall of the incubator. The compensation value then will be calculated with the formula. The camera thermal noise will be accepted as minimum noise value and considered in further process. The offset error is assumed to be a fix error and will be compensated in the pre-processing.

F. Thermal Noise Compensation and Temperature Value Calculation

The raw data from the FLIR camera is in 16-bit unsigned integer format. The raw data value range is 0-65535 and the actual temperature range is -20 °C to 120 °C, which results in a resolution of 0.00214°C. FLIR SC305 infrared camera datasheet shows an accuracy of ±2 °C or 2% of the temperature reading of the camera. There are couple steps to calculate the temperature value from the raw data as shown in

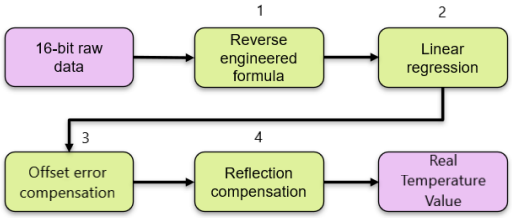

Fig. 6. Flow chart of temperature calculation with thermal noise compensation.

the flow chart in Fig. 6 to make the temperature reading more accurate.

1- The formula used by FLIR software to calculate the temperature data is owned by FLIR and not disclosed to the public. By reversed engineering formula infrared camera's output is being converted to real temperature. However, the temperature readings using reverse engineered formula has been slightly different compared to the FLIR ResearchIR software calculation. 2- By applying linear regression small difference in reading is being compensated. 3- The offset error introduced by drift in calibration in the camera is being compensated by comparing the calculation result with a measurement using PT100 temperature sensor. 4- By applying reflection compensation measured by a sensor attached to the incubator wall the final temperature reading is achieved with an accuracy of ±0.01 °C.

ACKNOWLEDGMENTS

The authors would like to thank the students who have contributed to this work, in particular Erik Wirianto who gave support on the experiments to gather results for this project.

REFERENCES

[1] Abbas, A. K., Heimann, K., Blazek, V., Orlikowsky, T., & Leonhardt, S. (2012). Infrared Physics & Technology, 55(6), 538–548.

[2] World Health Organization. Preterm Birth. https://www.who.int/news-room/fact-sheets/, detail/preterm-birth. 2018.

[3] Fluhr, J.W.,Darlenski, R., Taieb, A.,Hachem, J.-P., Baudouin, C., Msika, P., Berardesca, E. (2010). Functional skin adaptation in

infancy - almost complete but not fully competent. Experimental Dermatology, 19(6), 483–492. https://doi.org/10.1111/j.1600-0625.2009.01023.x

[4] Baharestani MM. (2007). An overview of neonatal and pediatric wound care knowledge and considerations. Ostomy/wound Management. Jun;53(6):34-6, 38, 40, passim.

[5] Lloyd, R., Goulding, R., Filan, P., & Boylan, G. (2015). Overcoming the practical challenges of electroencephalography for very preterminfants in the neonatal intensive care unit. Acta Paediatrica, 104(2), 152–157. https://doi.org/10.1111/apa.12869.

[6] Lund, C. H., Nonato, L. B., Kuller, J. M., Franck, L. S., Cullander, C., & Durand, D. K. (1997). Disruption of barrier function in neonatal skin associated with adhesive removal. The Journal of Pediatrics, 131(3),367–372. https://doi.org/10.1016/s0022-3476(97)80060-1.

[7] Rutter, N. (1987). Percutaneous Drug Absorption in the Newborn: Hazards and Uses. Clinics in Perinatology, 14(4), 911–930. https://doi.org/10.1016/s0095-5108(18)30740-1.

[8] VIVIER, P. M., LEWANDER,W. J., MARTIN, H. F., & LINAKIS, J. G. (1994). Isopropyl alcohol intoxication in a neonate through chronic dermal exposure: A complication of a culturally-based umbilical care practice. Pediatric Emergency Care, 10(2), 91–93. https://doi.org/10.1097/00006565-199404000-00008.

[9] Smith, J., Alcock, G., & Usher, K. (2013). Temperature Measurement in the Preterm and Term Neonate: A Review of the Literature.

[10] Neonatal Network, 32(1), 16–25. https://doi.org/10.1891/0730-0832.32.1.16.

[11] Acolet, D. (2005). Project 27/28: Inquiry Into Quality of Neonatal Care and Its Effect on the Survival of InfantsWhoWere Born at 27 and 28Weeks in England,Wales, and Northern Ireland. PEDIATRICS, 116(6). 1457–1465. https://doi.org/10.1542/peds.2004-2691.

[12] World Health Organization. Thermal Protection of the Newborn https://www.who.int/maternal_child_adolescent/documents/ws42097th/en/ 1997.

[13] Smith, J. (2014). Methods and Devices of Temperature Measurement in the Neonate: A Narrative Review and Practice Recommendations. Newborn and Infant Nursing Reviews, 14(2), 64–71.

https://doi.org/10.1053/j.nainr.2014.03.001

[14] Uslu, S., Ozdemir, H., Bulbul, A., Comert, S., Bolat, F., Can, E., & Nuhoglu, A. (2011). A Comparison of DifferentMethods of TemperatureMeasurements in Sick Newborns. Journal of Tropical Pediatrics, 57(6), 418–423. https://doi.org/10.1093/tropej/fmq120

[15] Rosenthal, H. M., & Leslie, A. (2006). Measuring temperature of NICU patients – A comparison of three devices. Journal of Neonatal Nursing, 12(4), 125–129. https://doi.org/10.1016/j.jnn.2006.05.007

[16] El-Radhi, A. S. (2006). Thermometry in paediatric practice. Archives of Disease in Childhood, 91(4), 351–356. https://doi.org/10.1136/adc.2005.088831

[17] Mcallister, T. A., Marshall, A., Roud, J. A., Holland, B. M., & Turner, T. L. (1986). OUTBREAK OF SALMONELLA EIMSBUETTEL IN NEWBORN INFANTS SPREAD BY RECTAL THERMOMETERS. The Lancet, 327(8492), 1262–1264. https://doi.org/10.1016/s0140-6736(86)91397-8

[18] Chardon, K., Cardot, V., Léké, A., Delanaud, S., Bach, V., Dewasmes, G., & Telliez, F. (2006). Thermoregulatory Control of Feeding and Sleep in Premature Infants. Obesity, 14(9), 1535–1542. https://doi.org/10.1038/oby.2006.177

[19] Hobbie, R. K., & Roth, B. J. (2015). Intermediate Physics for Medicine and Biology. https://doi.org/10.1007/978-3-319-12682-1

[20] Abbas, Minkina, W. & Dudzik, S. (2009). Infrared thermography : errors and uncertainties. Chichester, U.K: J. Wiley.

[21] Lytle, J. D.,Wilkerson, G.W., & Jaramillo, J. G. (1979).Wideband optical transmission properties of seven thermoplastics. Applied Optics, 18(11), 1842. https://doi.org/10.1364/ao.18.001842

[22] Bouguet, J. 1999. Pyramidal implementation of the lucas kanade feature tracker.

[23] Gunnar Farneback. 2003. Two-frame motion estimation based on polynomial expansion, Lecture Notes in Computer Science, (2749), 363-370.

[24] Mills, A., & Coimbra, Carlos F.M. (2015). Basic heat and mass transfer (Third ed.). San Diego, California: Prentice Hall.

[25] Nunak, T., Rakrueangdet, K., Nunak, N. & Suesut, Taweepol. (2015). Thermal Image Resolution on Angular EmissivityMeasurements using Infrared Thermography. Lecture Notes in Engineering and Computer Science. 1. 323-327.